NASA Contractor Report 182033

POWER FLOW ANALYSIS OF TWO COUPLED PLATES WITH ARBITRARY CHARACTERISTICS

J. M. Cuschieri

FLORIDA ATLANTIC UNIVERSITY
Center for Acoustics and Vibration
Department of Ocean Engineering
Boca Raton, Florida

Grant NAG1-685
June 1990

National Aeronautics and Space Administration

Langley Research Center
Hampton, Virginia 23665-5225

FOREWORD

This report describes the work performed during the second-half of the second year of the research project sponsored by NASA Langley-Research Center under Research Contract NAG-1-685, entitled, "Use of Energy Accountancy and Power Flow Techniques for Aircraft Noise Transmission". The author would like to acknowledge the financial support by NASA Langley through the Acoustics Division. Also, special thanks to the graduate assistants who worked on this project and to the Department of Ocean Engineering at Florida Atlantic University

During this second half of the second year, two Masters' thesis were completed with titles, "Power Flow Analysis of Simple Structures" and "Transmission of Vibrational Power in Joined Structures". The abstracts of these two Master thesis have been submitted for publication in the Journal of the Acoustical Society of America in the Technical Notes and Research Briefs Section.

Submitted by

J.M. Cuschieri

Principal Investigator

THIS PAGE INTENTIONALLY LEFT BLANK

ABSTRACT

In the last progress report (February, 88) some results were presented for a parametric analysis on the vibrational power flow between two coupled plate structures using the mobility power flow approach. The results reported then were for changes in the structural parameters of the two plates, but with the two plates identical in their structural characteristics. In this report this limitation is removed. The vibrational power input and output are evaluated for different area ratios, plate thickness ratios, and for different values of the structural damping loss factor for the source and receiver plates. In performing this parametric analysis, the source plate characteristics are kept constant. The purpose of this parametric analysis is to determine the most critical parameters that influence the flow of vibrational power from the source plate to the receiver plate. In the case of the structural damping parametric analysis, the influence of changes in the source plate damping is also investigated. The results obtained from the mobility power flow approach are compared to results obtained using a Statistical Energy Analysis (SEA) approach. The significance of the power flow results are discussed together with a discussion and a comparison between the SEA results and the mobility power flow results. Furthermore, the benefits derived from using the mobility power flow approach are examined.

1. INTRODUCTION

Previous work dealing with the use of the mobility power flow approach for the analysis of two coupled plate structures joined along a line junction [1,2], treated the extension of this technique to line connections. This represents an improvement on earlier work on the mobility power flow method [3,4] where only point contacts, hence mobility functions defined for single point location, were used. While the first work defined the mobility power flow approach and its advantages when used for structural dynamic analysis, and the more recent work extended the technique to the two dimensional case. In this later work a restriction was imposed on the type of analysis that can be performed; namely that the two plate structures used in the analysis must be identical. Thus, some generalizations are required to allow for the analysis of coupled plate structures when the two plates are not identical. These generalizations are addressed in this report. As anticipated, these generalizations increased the complexity of the expressions and the required computation time. However, the advantages of the mobility power flow technique over other methods of analysis in the mid-frequency range still hold.

With these generalizations, the mobility functions at the joint are completely defined; that is line mobilities have been obtained as a modal sum with a weighting function based on the location of the excitation. Any combination of plate structures can now be considered. Additionally, what has been derived for the L-shaped plate holds equally well for two plates joined along

a common boundary in a flat configuration, with a rigid line stiffener all along the joint between the two plates. Two alternate uses can be made of this mobility power flow approach. One alternative would be as a parametric analysis, similar to what is being presented in this report, to optimize the parameters that control the flow of vibrational power between the source plate and the receiver plate. In this case the influence of a flexible stiffener can be investigated by introducing additional mobility functions at the joint. The second alternative would be to consider the problem of multiple connected plate structures forming a periodic or quasi periodic structure. Although this may require more of an effort to formulate the problem, the approach is similar to that of two connected structures with the exception that all the power flow equations would be written in matrix form. For perfectly periodic structures, the mobility power flow approach would be very efficient since the mobility functions for each subelement of the periodic structure need only be evaluated once for just one of the spans. In the periodic structure analysis it would be useful to transform the analysis from the space domain to the wavenumber domain in the direction along the joints to simplify the representation. With this transformation, the analysis becomes identical to that of a one dimensional periodic structure with point junctions except that an inverse transform back to the space domain would be required.

The issues mentioned above are the topic of this progress report and thus it consists of two sections. The next section deals with the generalization of previous power flow results [2] to deal with plates of different structural characteristics including a parametric analysis. Results are presented for plates with four different area ratios, five different thickness ratios and six conditions of different structural damping. These results are compared to SEA results. In the following section, the development of the mobility power flow approach for the case of multiple connected structures is presented. If a transform is used, the same type of analysis applies to point or line joints. The formulation and results of this section are restricted to periodic beams with different number of spans and different characteristics for the stiffeners defining the spans.

2. MOBILITY POWER FLOW

In the development of the power flow expression for two coupled plates (figure 1) - equations (14) and (15) in [2] - it was assumed that the coupled plates were identical. This led to the simplification in evaluating the transferred vibrational power P_{trans} that,

$$\dot{\theta}_3 = \frac{-M_3}{M_2 + M_3}\,\dot{\theta}_F = \frac{-\dot{\theta}_F}{2} \qquad (1)$$

where M_2 and M_3 are the line mobilities at the joint for the source plate and the receive plate respectively, $\dot{\theta}_F$ is the angular velocity at the junction of the source plate due to the application of the excitation when the source plate is uncoupled from the receiver plate and $\dot{\theta}_3$ is the angular velocity at the junction of the receiver plate when coupled to the source plate. The simplification in equation (1) comes about since, for identical plates, $M_2 = M_3$. As a consequence of this result (equation 1) the integral for the transferred power over the entire length of the junction

$$P_{trans} = \frac{1}{2} \int_o^a \text{Real} \left\{ T^*(x) \quad \dot{\theta}_3(x) \right\} dx \tag{2}$$

can be evaluated analytically. The two summations for $T(x)$ and $\dot{\theta}_3(x)$

$$T(x) = \sum_{n=1}^{\infty} T_n^* \sin \left[\frac{n\pi x}{a} \right] \tag{3}$$

$$\dot{\theta}_3(x) = \sum_{n=1}^{\infty} \dot{\theta}_{F_n} \sin \left[\frac{n\pi x}{a} \right] \tag{4}$$

when multiplied and integrated over x, due to orthogonality, reduce to a single summation over n.

For plates with different structural characteristics, equation (1) does not hold and thus the integration cannot be done analytically. This also means that M_2 and M_3 must be completely defined. Starting with an expression for the moment distribution along the junction, from equations (A.14), (A.16) and (A.17) in reference [2], the moment distribution, normalized with respect to the applied excitation force F is given by

$$\frac{T(x)}{F} = \frac{4\,f}{ab_1^2}\sqrt{\frac{D_1^*}{\rho_1 h_1}}\sum_{n,m}^{\infty}\frac{(-1)^m\, m\, \sin\left(\frac{n\pi x_o}{a}\right)\sin\left(\frac{m\pi y_o}{b_1}\right)\sin\left(\frac{n\pi x}{a}\right)}{\left[\left(f_{n,m}^*\right)^2 - f^2\right]\left[A + R\,B\right]} \qquad (5)$$

where

$$A = k_1 \coth\left(k_1 b_1\right) - k_2 \operatorname{cotg}\left(k_2 b_1\right)$$

$$B = k_1' \coth\left(k_1' b_2\right) - k_2' \operatorname{cotg}\left(k_2' b_2\right)$$

$$R = \left[\left(\rho_1 h_1 D_1^*\right) / \left(\rho_2 h_2 D_2^*\right)\right]^{1/2}$$

where f is the frequency, ρ_i, h_i, b_i, D_i^* are, the density, thickness, length and flexural rigidity of plate i for i = 1 or 2, "a" is the width of the plates and the junction $f_{n,m}^*$ is the n,m modal frequency, and k_1 and k_2 are defined by

$$k_1^2 = 2\ k_x^2 + k_y^2$$
$$k_2^2 = k_y^2 \qquad (6)$$

where k_x and k_y are the wavenumbers in the x and y directions. The wavenumbers with a prime in the expression for B above indicate that these pertain to the receiver plate, plate 2, while wavenumbers without the prime are for the source plate, plate 1.

An important feature to notice with regards to the moment expression (equation 5) is that while the moment can be expressed as a sum of contributions of sinusoidal terms, which come about because of the way in which the plate would deflect in rotation under uncoupled conditions, the terms are weighted by a set of sine functions, the values of which are controlled by the values of x_o and y_o. That is, the amplitude of the moment components are determined by the mode of vibration of the source plate, controlled by the location of the excitation force.

Using equation (5) for the moment distribution and substituting in equation (A.12) of reference [2], two expressions for the edge mobilities are obtained. The expressions for M_2 and M_3, defined as the ratio of angular rotation per unit applied moment, are similar with mainly a change of subscript from 1 to 2. The reason for this is that the influence of the moment distribution is the same in both cases. Thus

$$M_2(x) = \frac{-j}{2\sqrt{\rho_1 h_1 D_1^*}} \frac{\displaystyle\sum_{n,m}^{\infty} \left\{ \frac{(-1)^m \, m \, \sin\left(\frac{n\pi x_o}{a}\right) \sin\left(\frac{m\pi y_o}{b_1}\right) \sin\left(\frac{n\pi x}{a}\right)}{\left[\left(f^*_{n,m} \right)^2 - f^2 \right] \left[1 + R\, B/A \right]} \right\}}{\displaystyle\sum_{n,m}^{\infty} \left\{ \frac{(-1)^m \, m \, \sin\left(\frac{n\pi x_o}{a}\right) \sin\left(\frac{m\pi y_o}{b_1}\right) \sin\left(\frac{n\pi x}{a}\right)}{\left[\left(f^*_{n,m} \right)^2 - f^2 \right] \left[A + R\, B \right]} \right\}} \tag{7}$$

and

$$M_3(x) = \frac{-j}{2\sqrt{\rho_2 h_2 D_2^*}} \frac{\displaystyle\sum_{n,m}^{\infty} \left\{ \frac{(-1)^m \, m \, \sin\left(\frac{n\pi x_o}{a}\right) \sin\left(\frac{m\pi y_o}{b_1}\right) \sin\left(\frac{n\pi x}{a}\right)}{\left[\left(f^*_{n,m} \right)^2 - f^2 \right] \left[R + A/B \right]} \right\}}{\displaystyle\sum_{n,m}^{\infty} \left\{ \frac{(-1)^m \, m \, \sin\left(\frac{n\pi x_o}{a}\right) \sin\left(\frac{m\pi y_o}{b_1}\right) \sin\left(\frac{n\pi x}{a}\right)}{\left[\left(f^*_{n,m} \right)^2 - f^2 \right] \left[A + R\, B \right]} \right\}} \tag{8}$$

where A, B and R have the same definitions as in equation (5), and the same notation is used.

By combining equations (5), (7) and (8) together with equations from [2] into the power flow expressions,

$$\frac{P_{in}}{|F(f)|^2} = \frac{1}{2}\ \text{Real}\left\{ M_1 - \int_o^a \frac{M_{12}\, M_{21}(x)}{M_2(x)\, M_3(x)}\, dx \right\} \qquad (9)$$

and

$$\frac{P_{trans}}{|F(f)|^2} = \frac{1}{2} \int_o^a \left\{ \frac{M_{12}}{M_2(x)\, M_3(x)} \right\}^2 \text{Real}\left\{ M_3(x) \right\} dx \qquad (10)$$

and integrating this last expression over the length of the joint, the input and transmitted power can be evaluated for the case of two plates joined along a common edge, which is pinned, with the plates having different structural characteristics. By using equations (5), (7) and (8) the influence of plate area, thickness, damping, and material on the input and transmitted power can be investigated. The results of this parametric analysis and the comparison of results obtained using SEA are presented in the next section.

3. PARAMETRIC ANALYSIS RESULTS

The results presented in [1] using an SEA approach investigate changes in the power ratio, defined as the ratio of the power transmitted to the input power, with changes in the

area ratio, thickness ratio, damping ratio, and changes in the material type of the plates. The same parameters will be investigated here and results will be presented for the following conditions.

(a) Area ratios (defined as ratio of receiver plate area to source plate area): 0.25; 0.5; 1.0; 2.0.

(b) Thickness ratios (ratio of receiver plate thickness to source plate thickness): 0.125; 0.25; 0.5; 1.0; 2.0; 4.0.

(c) Damping (receiver plate damping loss factor source plate damping loss factor): 0.1/ 0.001; 0.01/ 0.001; 0.1/ 0.01; 0.001/ 0.01; 0.01/ 0.1; 0.001/ 0.1.

(d) Material types (receiver plate material/ source plate material): Aluminum/ Aluminum, Steel/Aluminum.

Together with the results obtained using the mobility power flow approach, the results from [1] using SEA are also presented for comparison. In all of the analysis, except where indicated, the following base conditions for the source plate are considered.

Density = 2710 kg/m^3; Thickness = 0.00635m;

length = 0.5m; Width = 1.0 m;

Poisson ratio = 0.33; Loss factor = 0.01;

Young's Modulus = 7.2E+10 N/m^2;

3.1 Influence of Area Variations

The results for changes in the ratio of the area of the two plates are shown in figures (2) and (3). The first observation

that can be made regarding these results is that as expected, as the area of the receiver plate increases, the number of modes of the coupled system increases (figure 2(a)). While as the area of the receiver plate decreases the number of modes decrease (figure 2(b)). Figure (4) is a reproduction of the results for the power ratio using an SEA approach which were presented in reference [1]. Comparing the results in figure (3) with the results in figure (4), there is in general a very good agreement between the two sets of results, in the sense that as the area ratio increases, the general level of the power ratio also increases. However, the exact value of the power ratio is dependent on frequency. That is, while the general level may decrease as the area ratio decreases, for those modes that can be associated with the receiver plate, a significant portion of the input power finds its way into the receiver plate. From figures (2(c)) and (3(c)) it can be observed that for the two modes, one just under 400 Hz and one at approximately 700 Hz, roughly equipartition of vibrational power exists between the source and the receiver plates.

3.2 Influence of Thickness Variations

The variations in the power flow results with changes in the thickness ratio are shown in figures (5) and (6). In general similar results are obtained in this case to those for changes in the plate areas except that is this case a peak in the general level of the power ratio is obtained in the region where the thickness ratio is close to unity. As the thickness ratio

decreases, the general level of the power ratio decreases because of the impedance mismatch. The number of modes of the receiver plate however increases and thus there is an increase in the number of coupled modes and at those frequencies which correspond to modes of the receiver plate, a significant amount of vibrational power is transferred between the source plate and the receiver plate. This is very well demonstrated in figure (6(f)), where, while the general level is low, there are peaks in the power ratio curve corresponding to the modes which can be attributed to the receiver plate. These general results are similar to those obtained using an SEA approach (figure 7).

As pointed out earlier in this subsection, the variations in the power ratio with changes in thickness differ from the variations associated with changes in area in that the power ratio decreases as the thickness ratio increases. Apart from this decrease in the power ratio, the number of modes also decrease (figure 5(a)). However, in this case as well, for those modes which belong to the receiver plate, the power ratio can be significant and if the receiver mode happens to be at a trough in the behavior of the source plate, almost all the vibrational power supplied to the source plate is transferred to the receiver plate. Figure (6(a)) is a good representation of this in that while the general level is low, there are two peaks in the power ratio curve where the transferred power is more then 50% of the input power. This type of result show the significance of using the mobility power flow method over other methods such as SEA,

where the averaged results can be misleading at particular frequencies.

3.3 Influence of Damping

The damping loss factor values that are selected for the analysis are similar to those used in the SEA results presented in [1]. Figure (8) represents the power input and power transfer curves and figure (9) shows the power ratio curves for the different damping loss factor values. In this case, there are no changes in the number of modes of the coupled system since the size and thickness of both plates remain constant. However, the curves exhibit some smoothing of the modes as the damping loss factor increases. An interesting point is that the smoothing of the power input and transferred curves occurs irrespective of whether the damping increases in the source plate or the receiver plate.

Comparing the results to the SEA results (figure 10), again there is good general agreement between the two sets of results. However, similar to the other parametric changes, significant fluctuations exist between the mean (SEA) results and the actual results. Contrary to what would be expected, the fluctuations between the mean results and the actual results for the power ratio do not always decrease with increases in the damping of any of the two plates. This again shows the importance of analysis techniques which do not produce averaged results since at any one frequency, the fluctuations from the mean averaged values can be significant. These fluctuations cannot be assumed to decrease in

amplitude by increases in the structural damping of the components of the structure, that is by increased interaction between the modes.

With regards to the meaning of the results, the power ratio exhibits values close to unity when the damping of the receiver plate is high compared to the damping of the source plate. Most of the input power, flows to the receiver plate structure. As the damping of the source plate increases less vibrational power flows into the receiver plate. In the case where the source plate damping is much higher than the receiver plate damping, the value of the power ratio is extremely low implying that only a small portion of the input power is transferred to the receiver plate. However at particular frequencies, such as at resonances of the receiver structure, the power ratio can still reach values higher than the general mean low level (figure 9(f)).

3.4 Influence of Structure Material

A set of results are obtained for changes in the material of one of the plate substructures. To be consistent with the SEA results in [1] and thus be able to compare the results from the two techniques, one other type of material is considered. Figures (11) and (12) show the results for the power input and output and the power ratio obtained using the mobility power flow technique, together with the results from SEA, for the case when the source plate substructure material is changed from aluminum to steel. Comparison between these results shows that for the mobility power flow predictions, the general level for the power

ratio remains approximately the same as that for the case when both plate substructures are of the same material. This is consistent with the SEA results. However, the exact detailed characteristics of the power ratio curve are different (figure 11(b)) as compared to the case for the same material (figure 3(b)). This is consistent with the results that have been presented using the mobility power flow approach.

The above results, for changes in area, thickness, damping and material, demonstrate a typical parametric analysis for two coupled structures using the mobility power flow approach. In performing the analysis, the evaluation of the mobility functions was very time consuming, but these evaluations need not be repeated for each change in the parameters of the global structure. Only those mobility functions which were effected by changes in the parameters of the substructures had to be re-evaluated. This made the analysis very efficient since, if the only parametric changes made are for the receiver plate, then only M_3 had to be re-evaluated. The remaining mobility functions were obtained from data files stored from previous evaluations of these functions. This efficiency makes the mobility power flow method a very attractive tool for structural analysis.

4. EXTENSION TO MULTIPLE CONNECTED STRUCTURES

In extending the mobility power flow techniques to line connected structures, it has been shown that the fundamental expression for the vibrational power input and output are not

different from those for point connected structures, except that the mobility functions are space variables as well as frequency variables, and for the transferred vibrational power the expression for the power is integrated over the entire length of the joint. Thus, in extending the mobility power flow method to multiple connected structures, one only needs to formulate the approach to one dimensional structures. The extension to two dimensional junctions follows the same as the example of the two coupled plate structures that have been presented.

Additionally, the results that have been obtained for the L-shaped beam [3] and the L-shaped plate hold equally well for two coupled plate or beam structures in a side by side configuration as shown in figure (13). This mobility power flow approach can, with an extension of this analysis to multiple coupled structures, be used to deal with periodic structures. The application of this mobility power flow technique to a periodic beam configuration with both rigid and flexible supports between the spans will be discussed in this section. In the case of flexible supports the formulation also shows how mobility elements can be introduced at the joints between the substructures to model such elements as stiffeners and dissipative junctions.

4.1 Basic Approach

Considering first a series of linearly coupled structures, (figure 14) where V_i (i = A, B, C, etc.) represent the motion of the junctions which may be rotational or translational and F_i (i

= A, B, C, etc) represent forces or moments that are transmitted across the junction. Since in all the previous analysis the power flow method has been restricted to point loading, it is assumed here that the coupled structure is excited by a point load on one of the substructures. Writing down the relationships for the velocities and the loads for each of the junctions of the multiple coupled structure.

$$V_1 = F_1 M_1 + F_A M_{12}$$

$$V_A = F_1 M_{21} + F_A M_2 = -F_A M_3 - F_B M_{34}$$

$$V_B = -F_A M_{43} - F_B M_4 = F_B M_5 + F_C M_{56}$$

$$\text{etc.} \qquad (11)$$

where F_1 is the input loading and M_j and M_{jk} represent respectively the input mobility functions and transfer mobility functions.

In the derivation of the equations for the solution of this multiple coupled structure, the number of substructures is limited to four. Also, instead of writing complete expressions for the input and transferred power between the substructures, the relationships are written in matrix form, which allow for the expansion of the solution to more than four substructures by adding terms in the matrices in the same pattern as those

identified with just four substructures. Thus, the matrix relationships for the velocities and forces for the four coupled substructures case are as follows:

$$\begin{bmatrix} (M_2 + M_3) & -M_{34} & 0 \\ -M_{43} & (M_4 + M_5) & -M_{56} \\ 0 & -M_{65} & (M_6 + M_7) \end{bmatrix} \begin{bmatrix} F_A \\ F_B \\ F_C \end{bmatrix} = \begin{bmatrix} M_{21} F_1 \\ 0 \\ 0 \end{bmatrix} \tag{12}$$

$$\begin{bmatrix} V_1 \\ V_A \\ V_B \\ V_C \end{bmatrix} = \begin{bmatrix} M_1 & -M_{12} & 0 & 0 \\ 0 & M_3 & -M_{34} & 0 \\ 0 & 0 & M_5 & -M_{56} \\ 0 & 0 & 0 & M_7 \end{bmatrix} \begin{bmatrix} F_1 \\ F_A \\ F_B \\ F_C \end{bmatrix} \tag{13}$$

and the power flow is given by

$$\begin{bmatrix} P_1 \\ P_A \\ P_B \\ P_C \end{bmatrix} = \frac{1}{2} \text{ Real } \left\{ \begin{bmatrix} V_1^* & 0 & 0 & 0 \\ 0 & V_A^* & 0 & 0 \\ 0 & 0 & V_B^* & 0 \\ 0 & 0 & 0 & V_C^* \end{bmatrix} \begin{bmatrix} F_1 \\ F_A \\ F_B \\ F_C \end{bmatrix} \right\} \tag{14}$$

where P_1 represents the power input and P_A, P_B, etc represent the power flow between the spans at junctions A, B, etc. respectively. The procedure for the solution would be to first

evaluate the junction loadings, F_A, F_B, etc. from equation (12) and use these values in equation (13) to solve for the velocities. Having obtained the velocities and the loadings at the junctions the power flow is evaluated using equation (14).

The above approach is applied to a periodic beam on rigid supports, with a transverse point load applied at the midpoint of the first span. The loadings F_A, F_B, etc., in this case would represent moments applied at the junctions and the velocities V_A, V_B, etc. would represent rotational velocities. The results for different number of spans are shown in figure (15). As would be expected, the introduction of the additional spans would create additional resonant modes. As the number of spans increases, the additional resonant modes start to merge to create the familiar pass bands and stop bands. This is very well demonstrated in figure (15(c)) for a 50 span perfectly periodic beam.

4.2 Periodic Beam on Flexible Supports

The above analysis is an extension of the results obtained for the L-shaped beam [3]. In that case, the number of resonant frequencies in each group of modes was two, corresponding to the two spans, as the number of spans increases, so does the number of resonant frequencies. Since the beam spans are on rigid supports, only rotational motion at the support has to be considered. In the case of flexible supports, to which one may associate both stiffness, inertia or damping, both translational and rotational motions need to be considered at the junctions. Thus, the number of mobility functions for each beam span will

increase; apart from the additional mobility terms to describe the support in translation and rotation.

Since mobility terms describe the support conditions, the end boundaries of the beams are free - free. Thus, considering the two spans shown in figure (16), the consistency expressions are (assuming that the support has no coupling between translational and rotational motion):

(a) sum of forces and moments at the support is zero

$$F_{A1} + F_{A2} = F_S$$
$$T_{A1} + T_{A2} = T_S \qquad (15)$$

where F_S and T_S are the support force and torque in the direction as shown in figure 16.

(b) Equal rotational and translation velocity for all components.

Using these consistency relationships, matrix expressions can be derived for the behavior and thus power flow. Because of the number of terms that are involved in the matrices, the expressions for a two span beam are shown here. The extension of these matrix expressions to more spans can be easily accomplished by following the same general pattern as can be identified in these matrix equations

$$\left[\begin{array}{ccccc|ccc}
M_1+M_s & M_{12} & 0 & 0 & -Q_1 & Q_{12} & 0 & 0 \\
M_{21} & M_2+M_s & M_s & 0 & -Q_{21} & Q_2 & 0 & 0 \\
0 & M_s & M_3+M_s & M_{34} & 0 & 0 & -Q_3 & Q_{34} \\
0 & 0 & M_{43} & M_4+M_s & 0 & 0 & -Q_{43} & Q_4 \\
\hline
-N_1 & N_{12} & 0 & 0 & L_1+M_s' & L_{12} & 0 & 0 \\
-N_{21} & N_2 & 0 & 0 & L_{21} & L_2+M_s' & M_s' & 0 \\
0 & 0 & -N_3 & N_{34} & 0 & M_s' & L_3+M_s' & L_{34} \\
0 & 0 & -N_{43} & N_4 & 0 & 0 & L_{43} & L_4+M_s'
\end{array}\right]
\left[\begin{array}{c} F_A \\ F_{B1} \\ F_{B2} \\ F_c \\ \hline T_A \\ T_{B1} \\ T_{B2} \\ T_c \end{array}\right]
=
\left[\begin{array}{c} -M_{1a} \\ -M_{1a} \\ 0 \\ 0 \\ \hline N_{ia} \\ -N_{1a} \\ 0 \\ 0 \end{array}\right]
\tag{16}$$

$$\left[\begin{array}{c} V_a \\ V_A \\ V_B \\ V_c \\ \theta_A \\ \theta_B \\ \theta_c \end{array}\right]
=
\left[\begin{array}{ccccccccc}
M_a & M_{ai} & M_{a2} & 0 & 0 & -Q_{ai} & -Q_{az} & 0 & 0 \\
0 & -M_s & 0 & 0 & 0 & 0 & 0 & 0 & 0 \\
0 & 0 & -M_s & -M_s & 0 & 0 & 0 & 0 & 0 \\
0 & 0 & 0 & 0 & -M_s & 0 & 0 & 0 & 0 \\
0 & 0 & 0 & 0 & 0 & -M_s' & 0 & 0 & 0 \\
0 & 0 & 0 & 0 & 0 & 0 & -M_s' & -M_s' & 0 \\
0 & 0 & 0 & 0 & 0 & 0 & 0 & 0 & -M_s'
\end{array}\right]
\left[\begin{array}{c} F \\ F_A \\ F_{B1} \\ F_{B2} \\ F_c \\ T_A \\ T_{B1} \\ T_{B2} \\ T_c \end{array}\right]
\tag{17}$$

where M, N, Q, and L are mobility functions defined by $M = V/F$; $N = \dot{\theta}/F$; $Q = V/T$ and $L = \dot{\theta}/T$. V is the translational velocity, $\dot{\theta}$ the rotational velocity, F is the translational force and T the torque. The single and double subscripts denote input and transfer mobilities as indicated in figure (16). M_S and $M_{S'}$ represent the translational and rotational mobility of the supports respectively.

The solution to these matrix equation for the velocities and junction forces and moments can be combined to give the power flow or power content of components of the periodic structure.

5. CONCLUSIONS

In this progress report the modifications necessary for the mobility power flow expressions to deal with two coupled plate structures with different structural characteristics have been presented. A number of results for a parametric analysis are compared to results obtained using an SEA approach. The results obtained using the mobility power flow approach represent details of the modal response both for the power input and power transferred curves as well as in the power ratio curves. Comparing these to the results obtained using an SEA approach, it can be observed that significant differences can be obtained between the actual results (represented by the mobility power flow results) and the mean level results obtained from an SEA analysis. These significant differences in the power ratio can be more pronounced in cases where the response of the global

structure is dominated by modes of the receiver substructure. Under such conditions, while the general level of the power ratio may be low, at particular frequencies ratios close to unity can be obtained.

Also presented in this report is a technique for applying the mobility power flow approach to the case of multi coupled structures. Matrix expressions and results are presented for a multiple span periodic beam with rigid supports, and the relevant expressions are derived for flexible supports. This analysis represents one application of the mobility power flow method which can be applied to both one dimensional and two dimensional junctions representing periodic beams and plates respectively.

In completing the analysis on the L-shaped plate, experimental measurements need to be performed to verify the analytical results. This will be the topic for the future work, after completing the analysis for distributed excitation on the source panel of the L-shaped plate. In performing this experimental analysis, it would be required that some development be achieved in measuring power flow near structural discontinuities without the use of a large number of transducers which would make the measurement cumbersome. This will be addressed in future work in this area.

REFERENCES

1. J. M. Cuschieri, "Parametric and Experimental Analysis Using a Power Flow Approach", NASA Contract Report 181990, February 1988.

2. J. M. Cuschieri, "Extension of Vibrational Power Flow Techniques to Two-Dimensional Structures", NASA Contract Report 181710, September 1988.

3. J. M. Cuschieri, "Power Flow as a Complement to Statistical Energy Analysis and Finite Element Analysis", ASME Publication NCA - Vol 3 (1987).

4. R. J. Pinnington, R. G. White (1981) Journal of Sound and Vibration 75, 179-197, "Power Flow Through Machine Isolators to Resonant and Non-Resonant Beams.

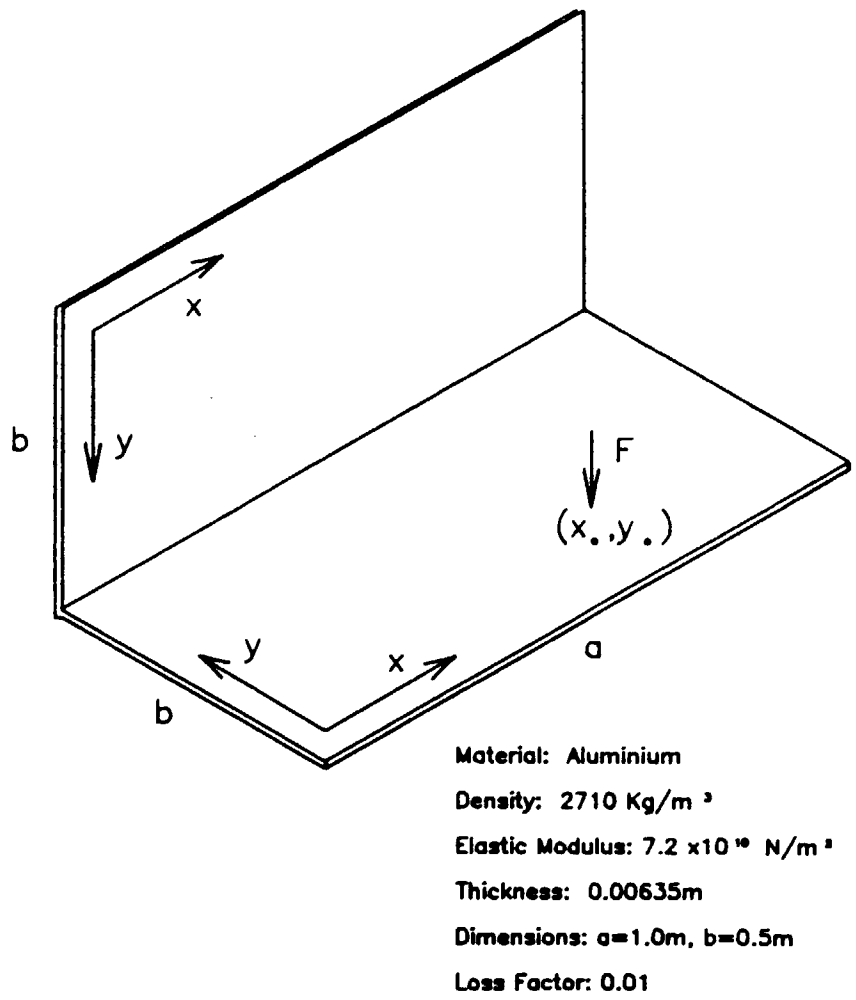

Figure 1. Plate structure showing plate characteristics.

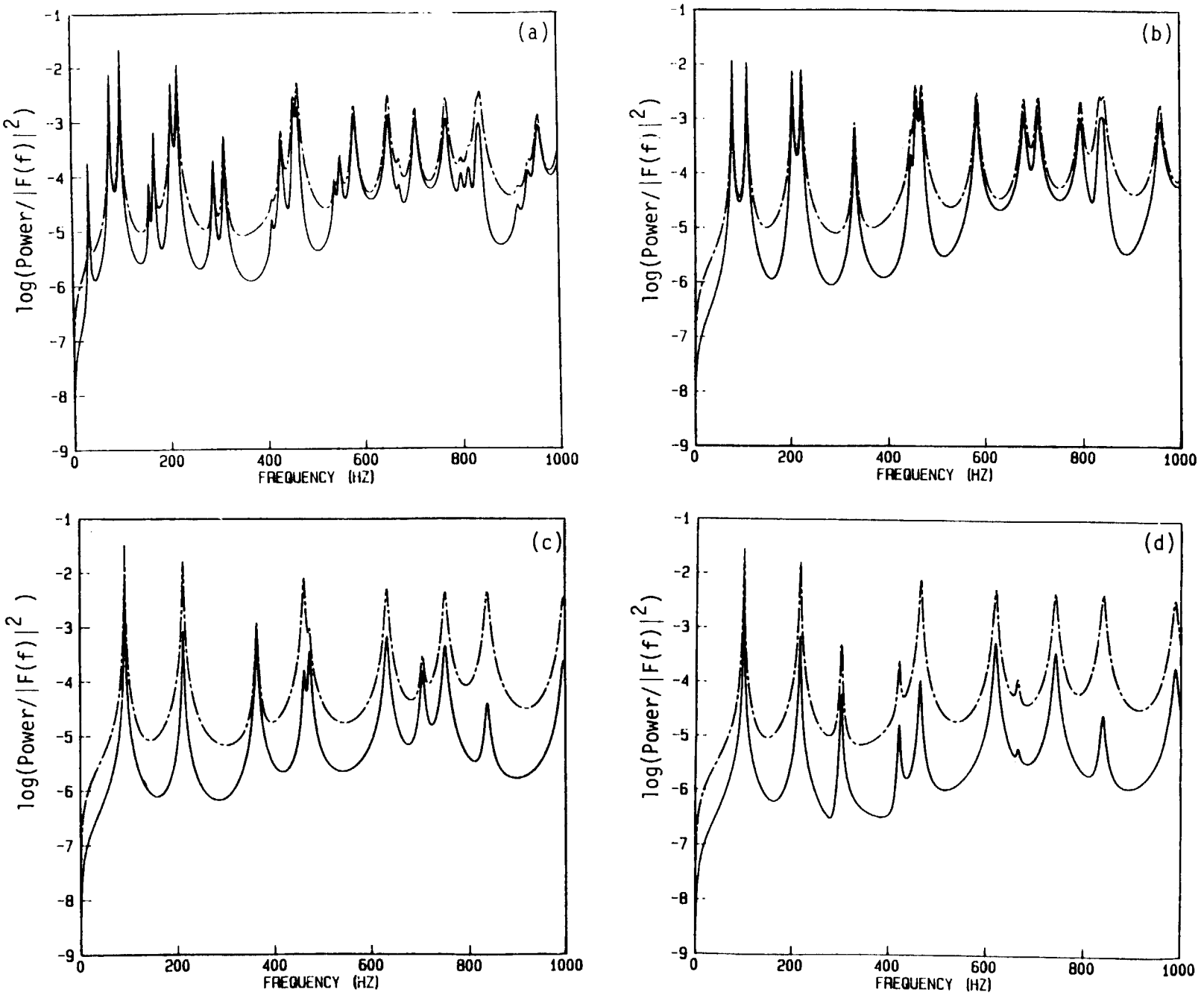

Figure 2. Power input and power transfer curves for different area ratios, using the mobility power flow, ___:power transfer; -.-.-: power input. (a) 2.0; (b) 1.0: (c) 0.5: (d) 0.25 .

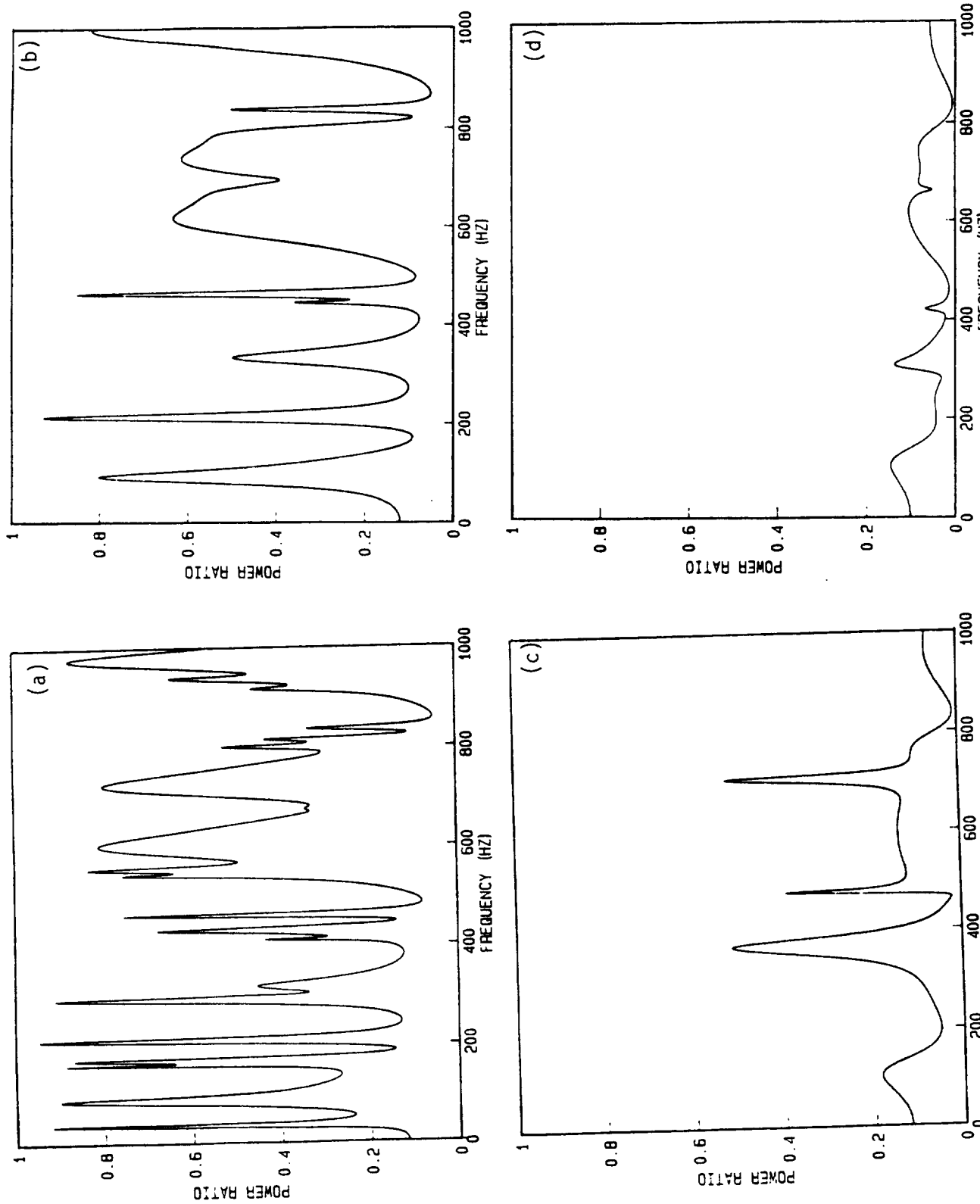

Figure 3. Power ratio curves for different area ratios, (a) 2.0; (b) 1.0; (c) 0.5; (d) 0.25 .

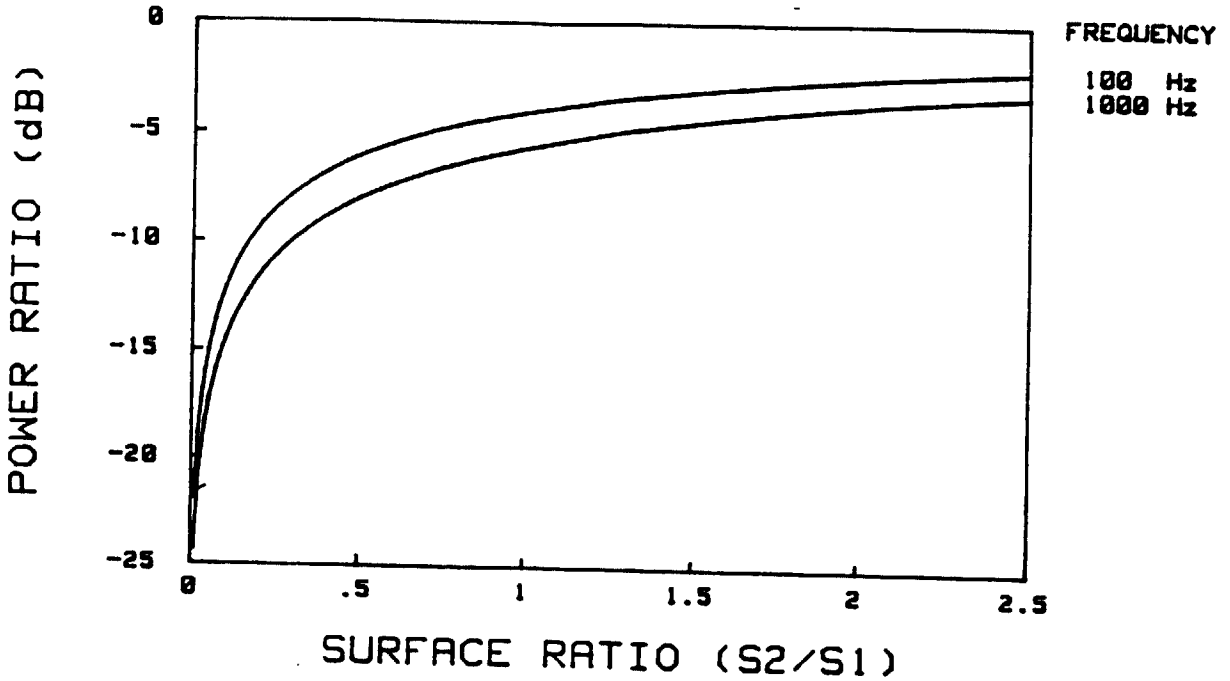

FIGURE 4. **Power Ratio as a Function of the Area Ratio** of the two plates using an SEA approach (reference 1).

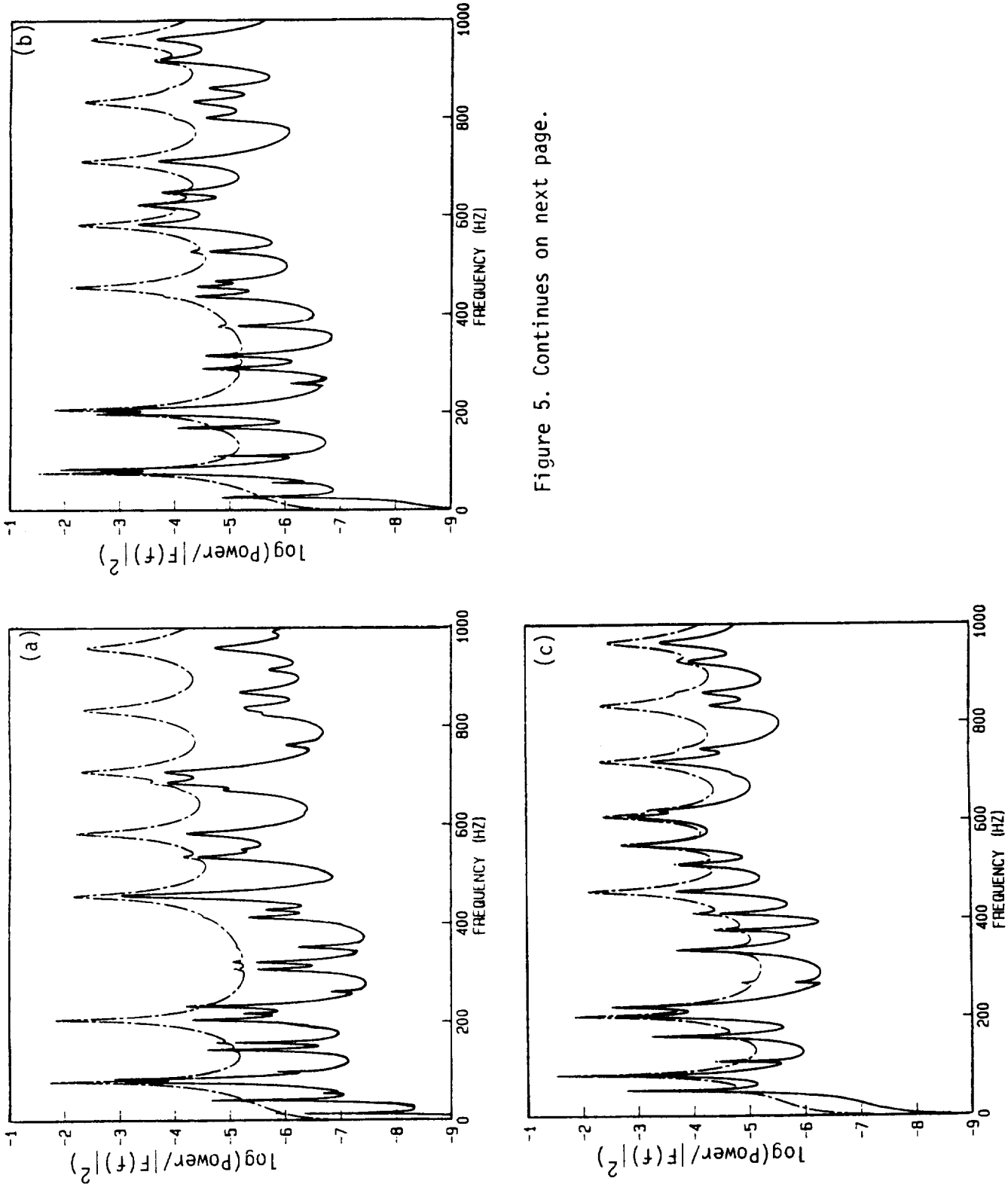

Figure 5. Continues on next page.

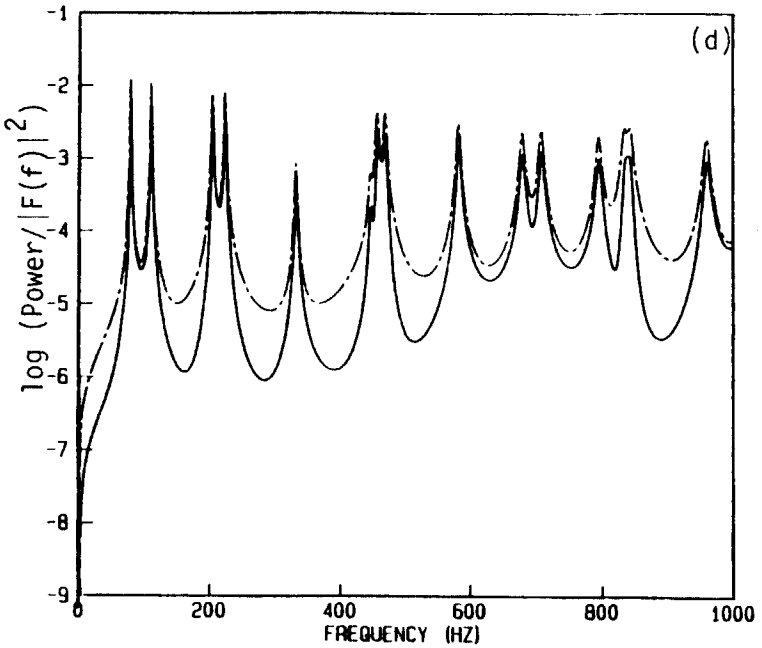

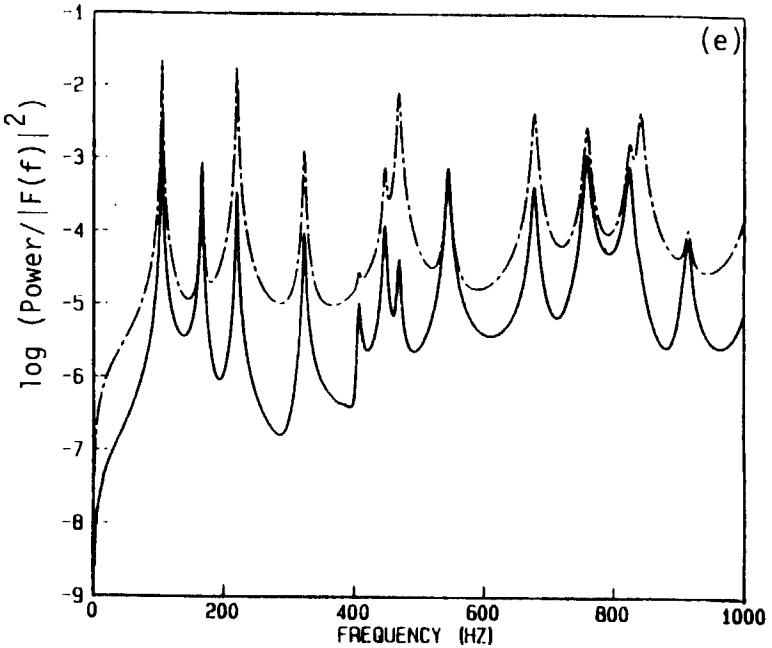

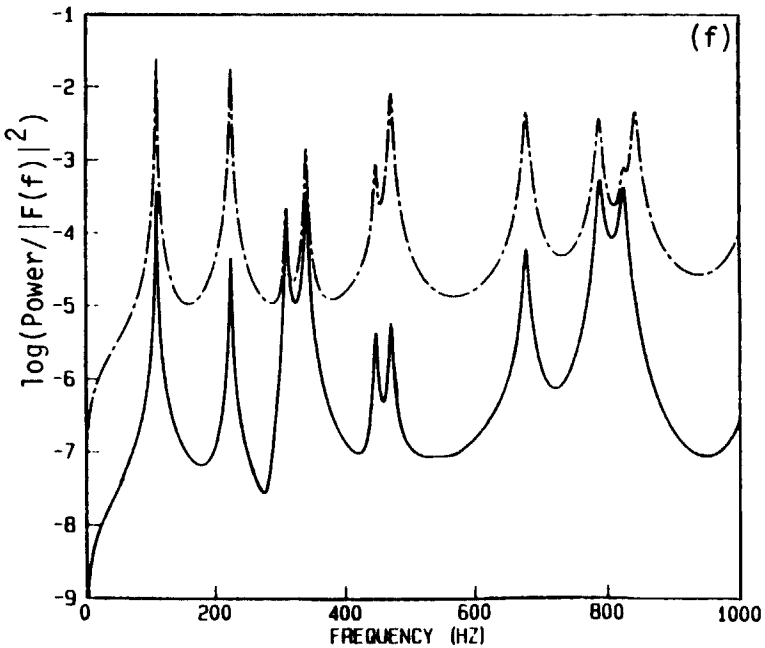

Figure 5. Mobility power flow results for the power input (-.-.-) and power transfer (___) for different thickness ratios. (a) 0.125; (b) 0.25: (c) 0.5: (d) 1.0: (e) 2.0; (f) 4.0 .

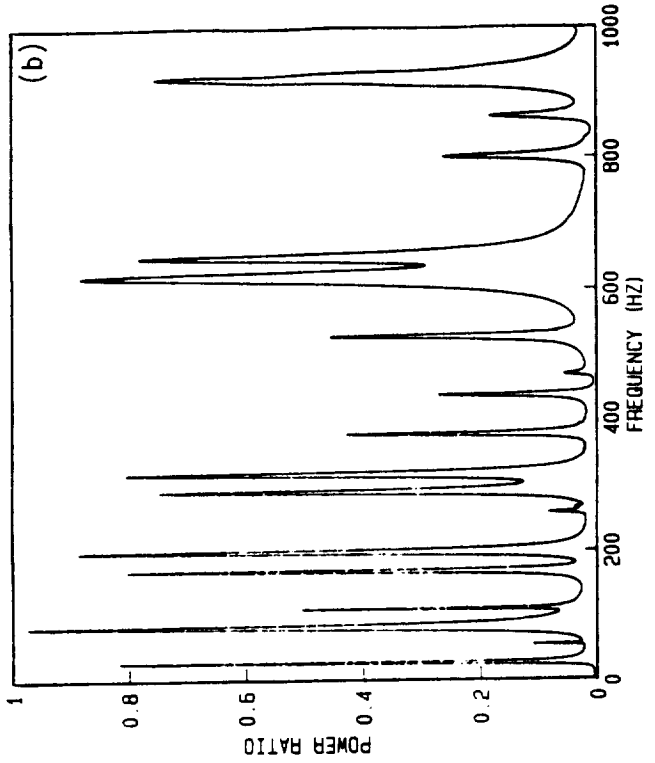

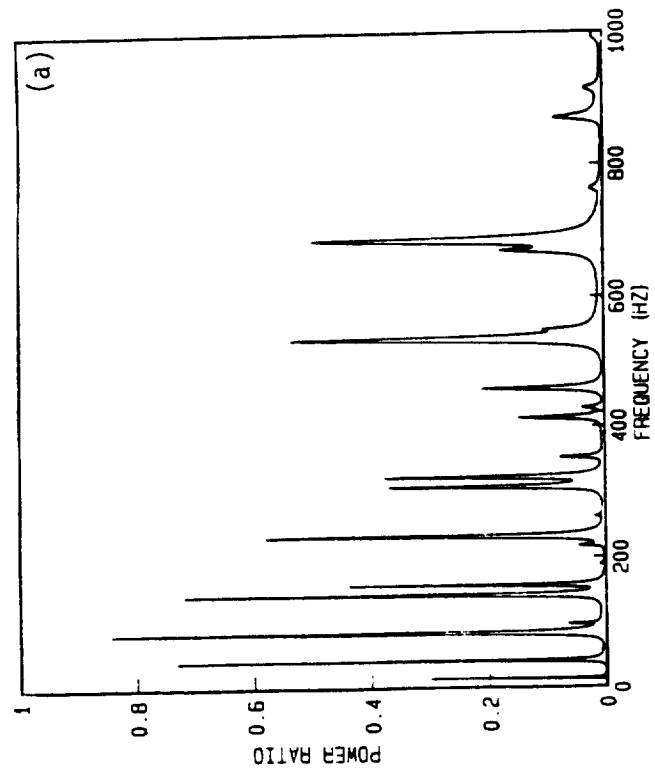

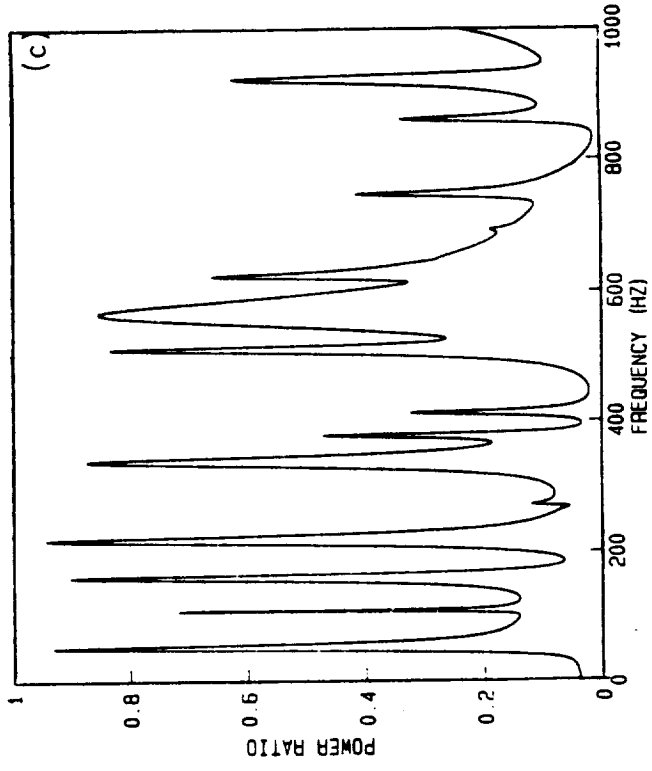

Figure 6. Continues on next page.

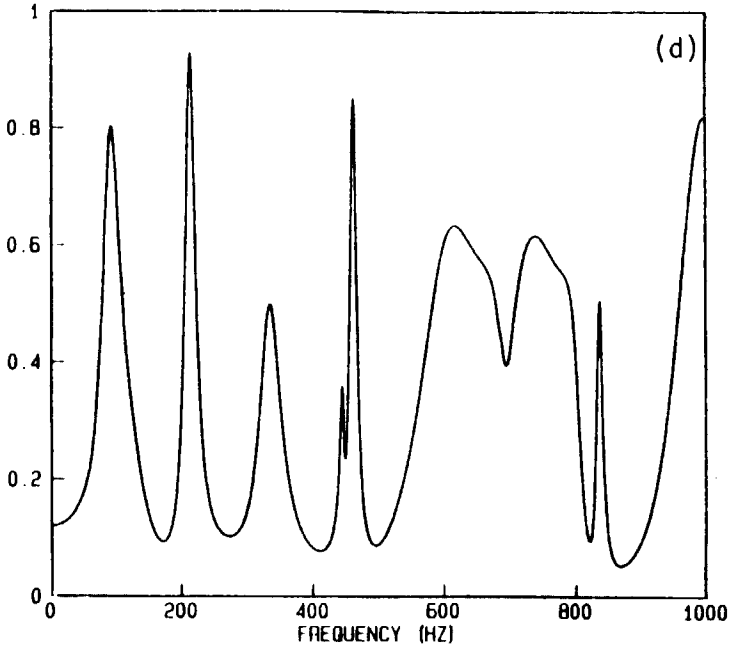

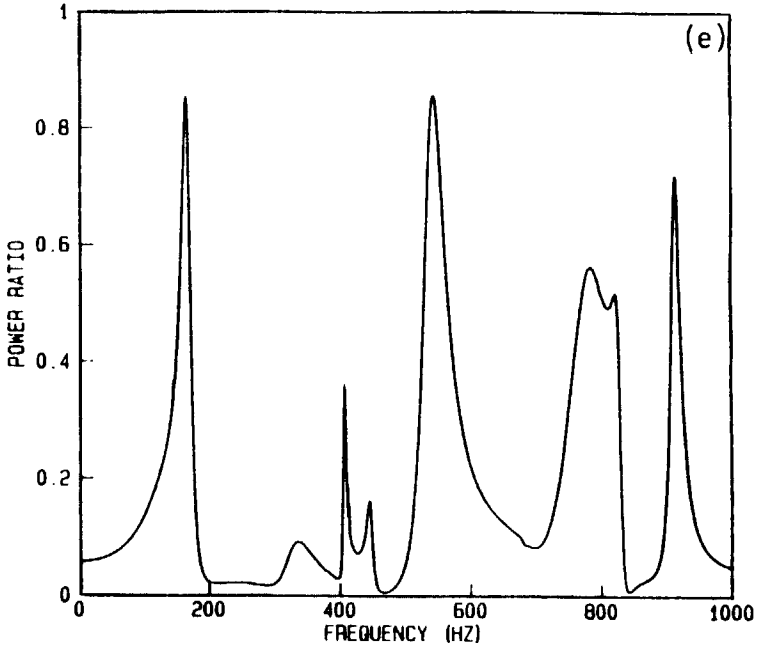

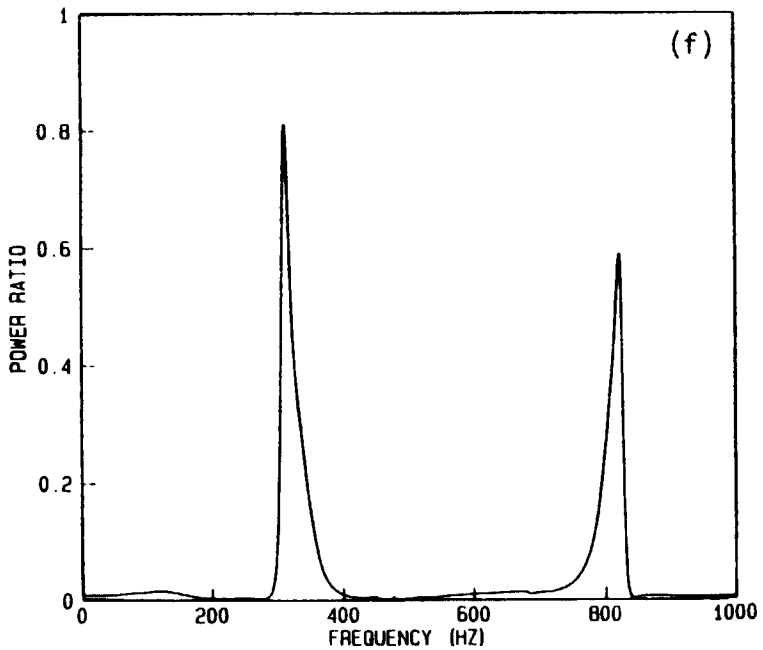

Figure 6. Power ratio results using the mobility power flow approach for different thickness ratios: (a) 0.125; (b) 0.25; (c) 0.5; (d) 1.0; (e) 2.0; (f) 4.0 .

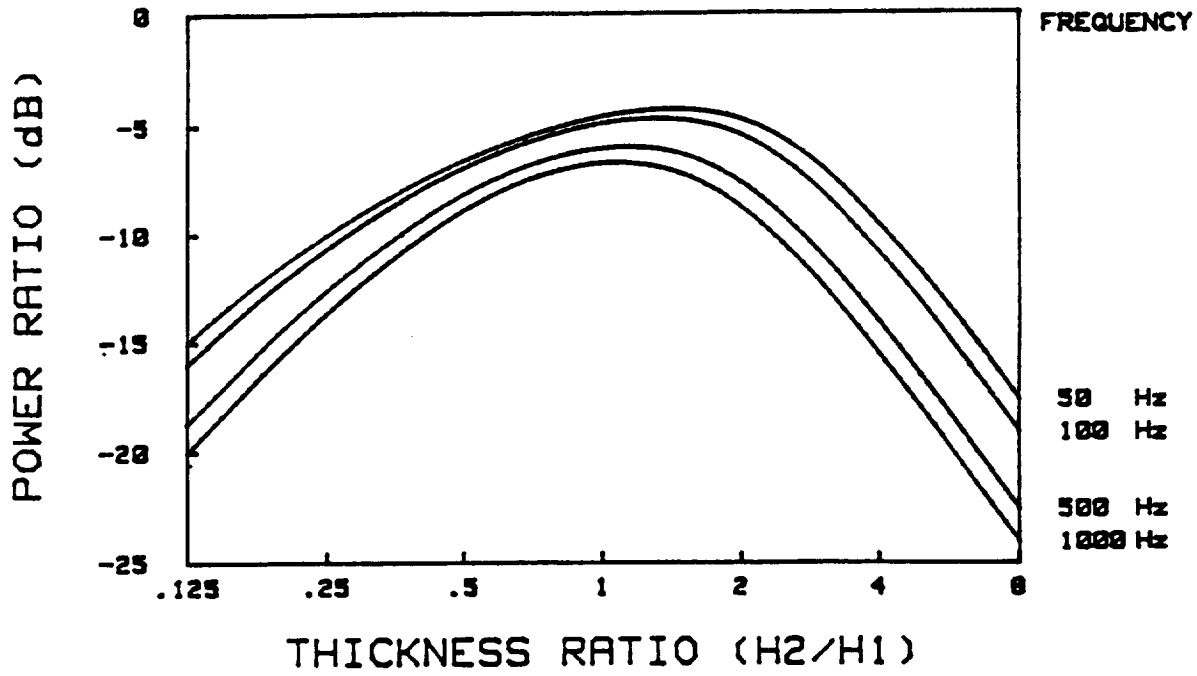

FIGURE 7. **Power Ratio as a Function of the Thickness Ratio** of two plates using SEA, (reference 1).

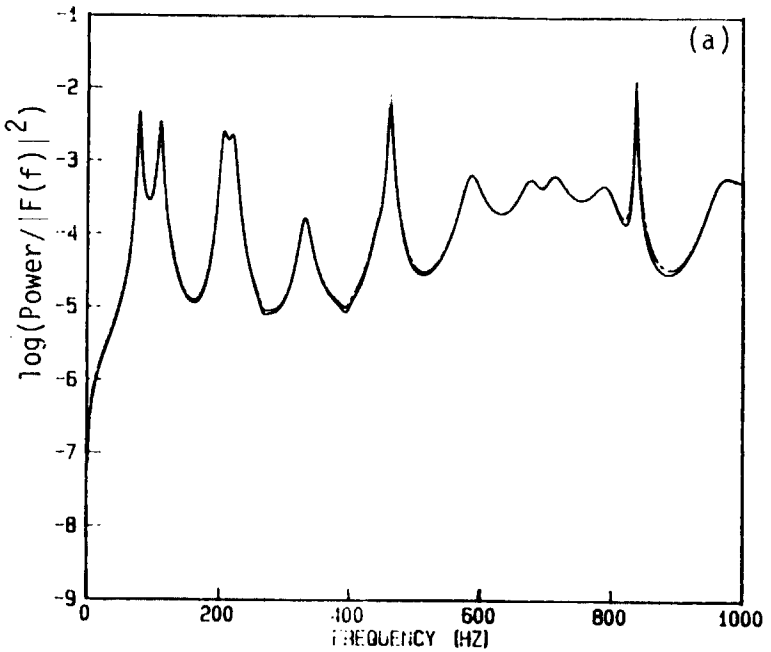

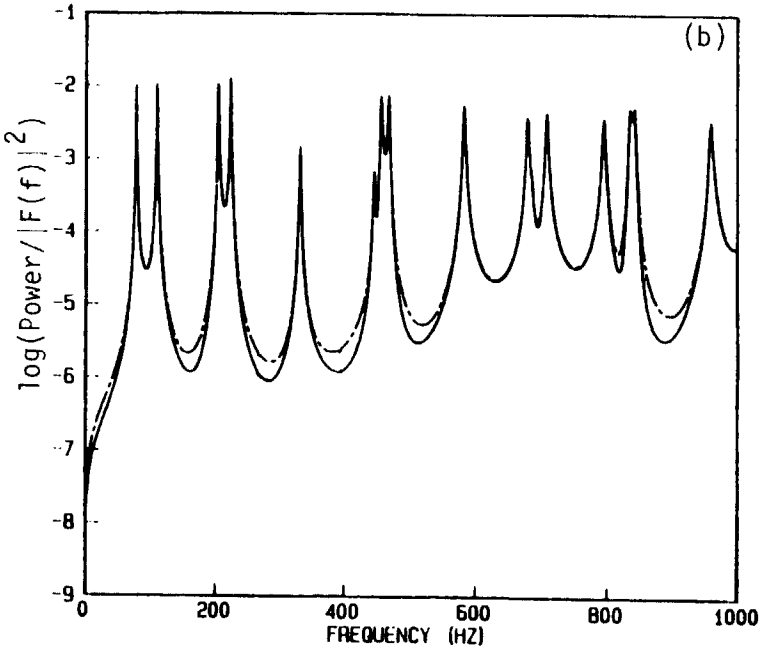

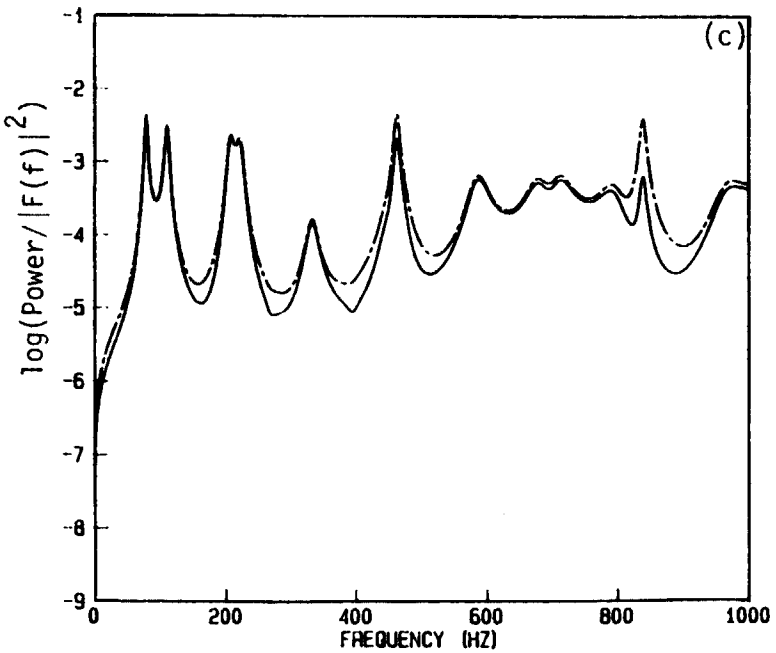

Figure 8. Continues on next page.

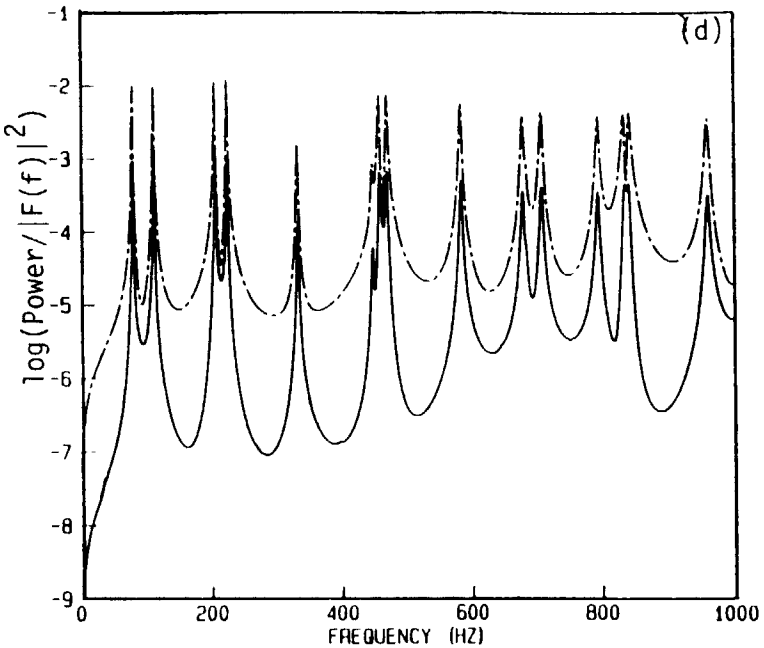

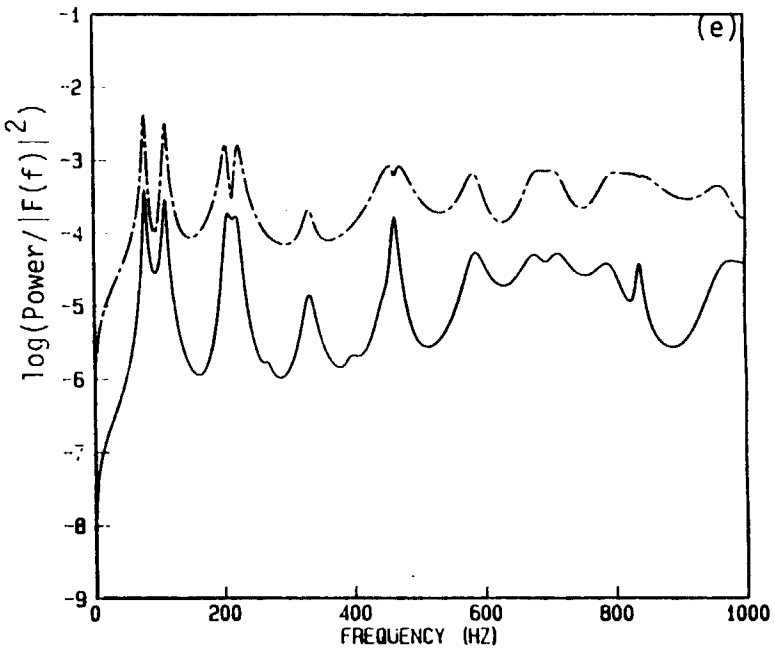

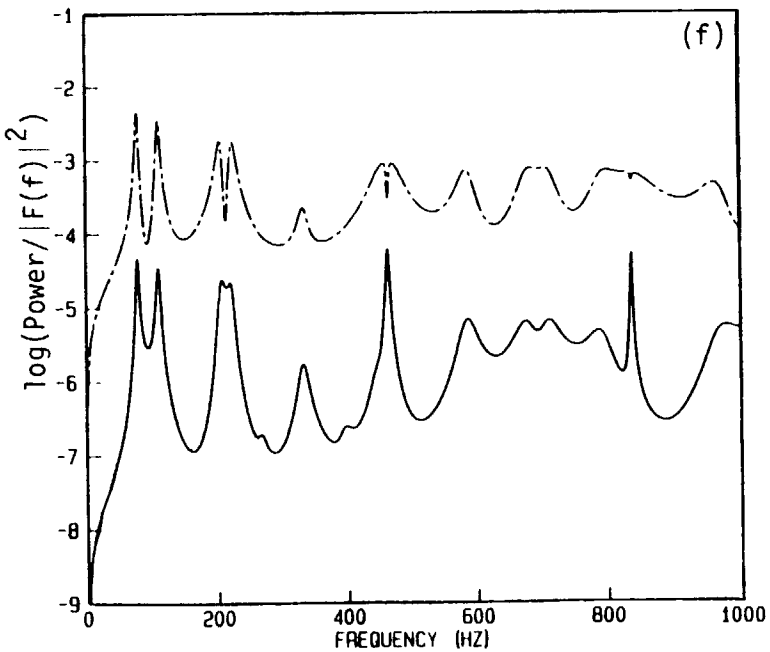

Figure 8. Power input (-.-.-) and power transfer (___) results using a mobility power flow approach for different damping loss factor of source and receiver plates respectively. (a) 0.001/0.1; (b) 0.001/0.01· (c) 0.01/0.1: (d) 0.01/0.001; (e) 0.1/0.01; (f) 0.1/0.001 .

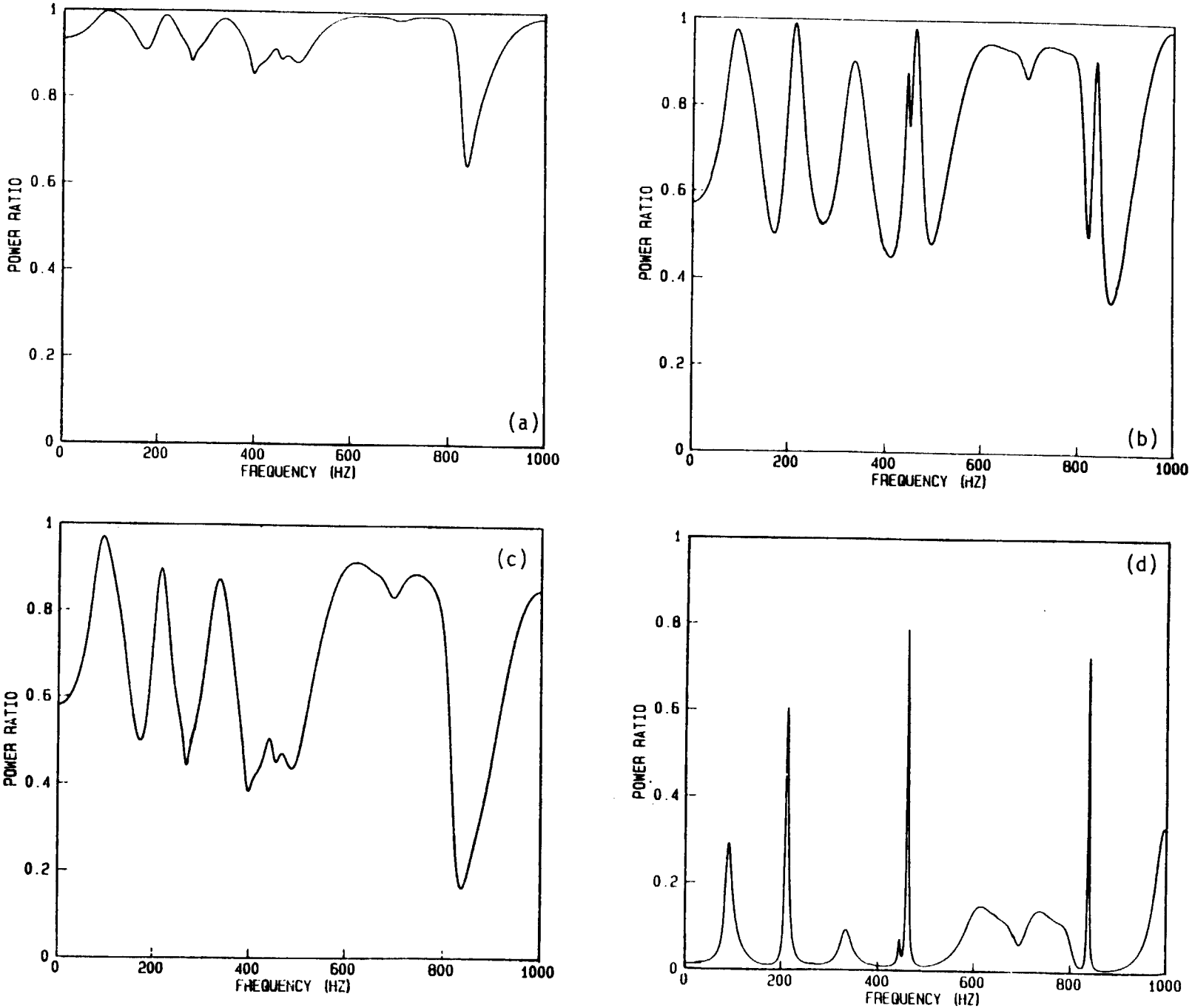

Figure 9. continues on next page.

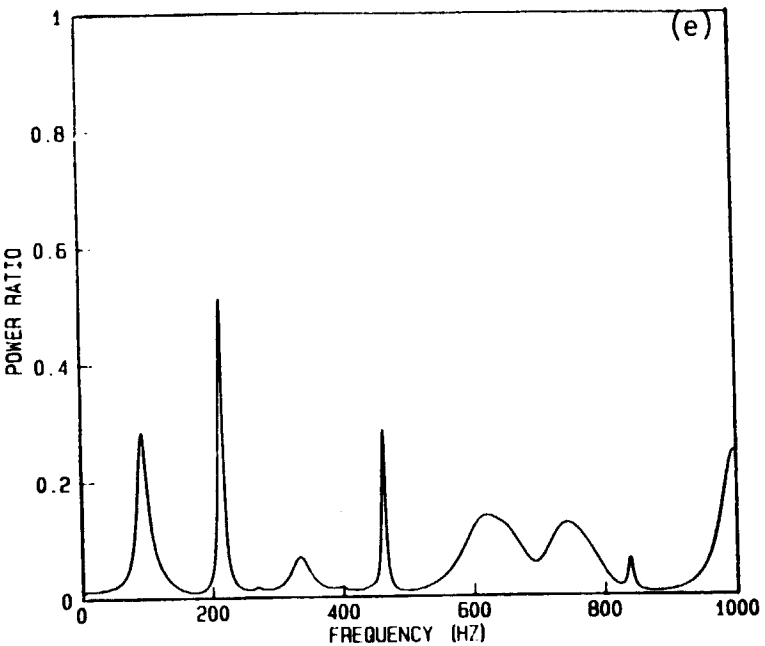

Figure 9. Power ratio results for different source and receiver plate damping loss fator. (a) 0.001/0.1; (b) 0.001/0.01: (c) 0.01/0.1: (d) 0.01/0.001: (e) 0.1/0.01; (f) 0.1/0.001 .

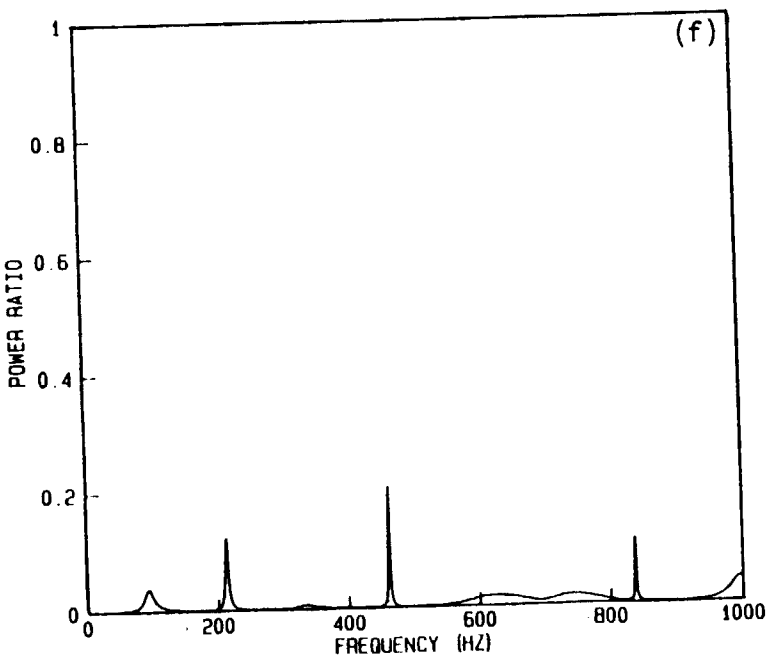

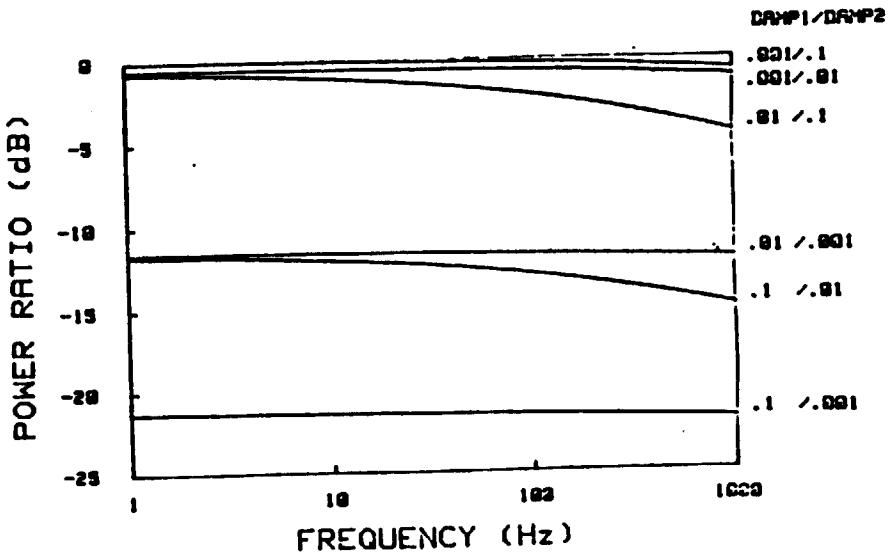

FIGURE 10. Power Ratio as a Function of Damping (plates with different damping).

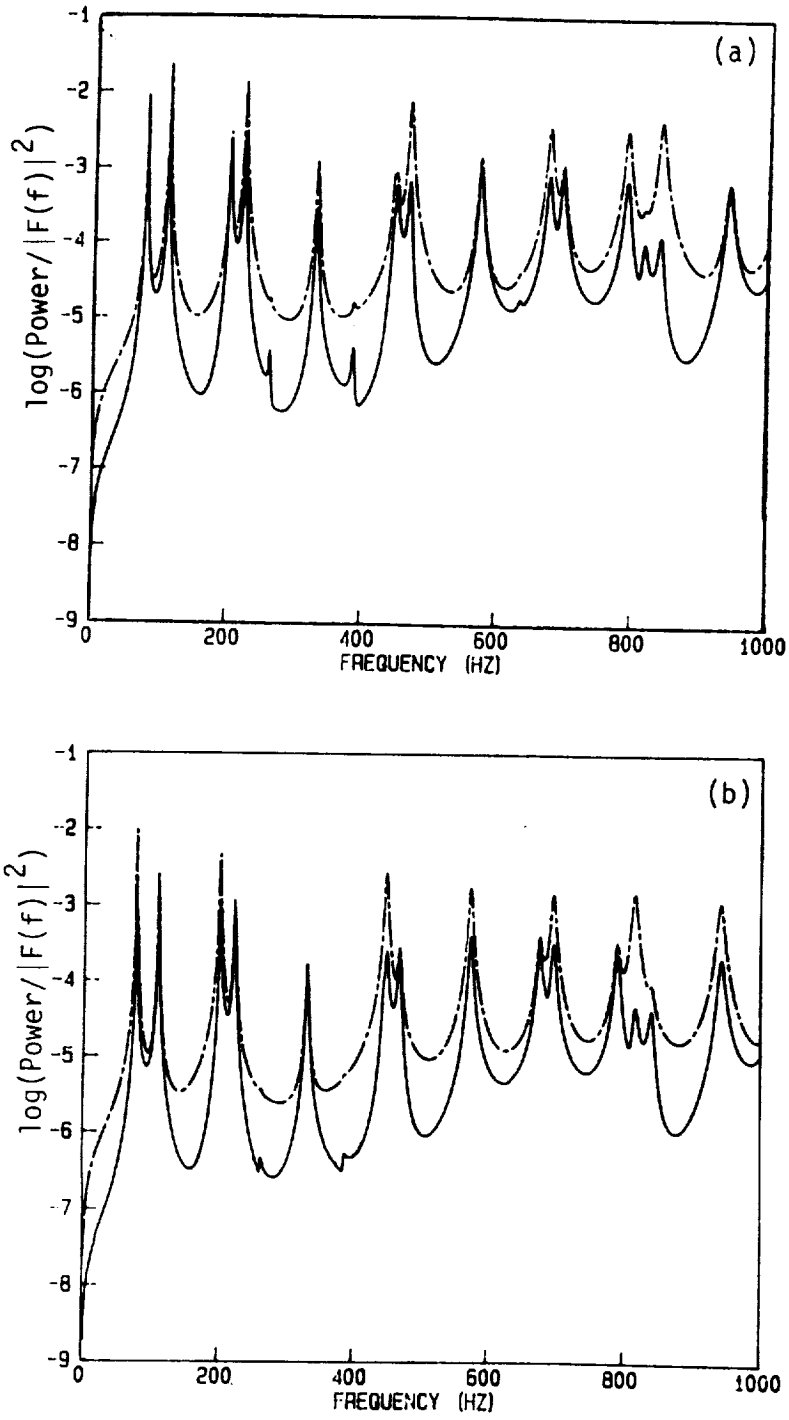

Figure 11. Power input (-.-.-) and power transfer (___) results for different source plate and receiver plate materials. (a) Aluminium/steel; (b) steel/aluminium.

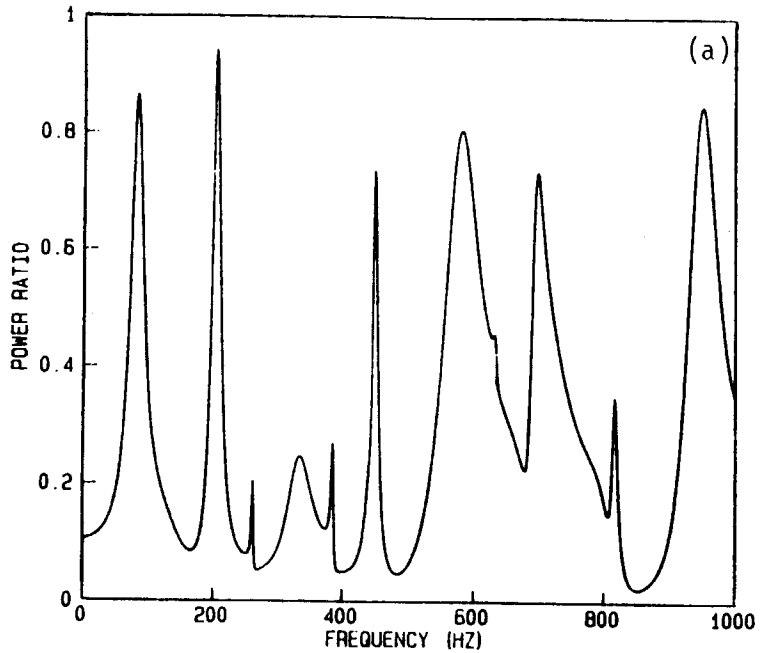

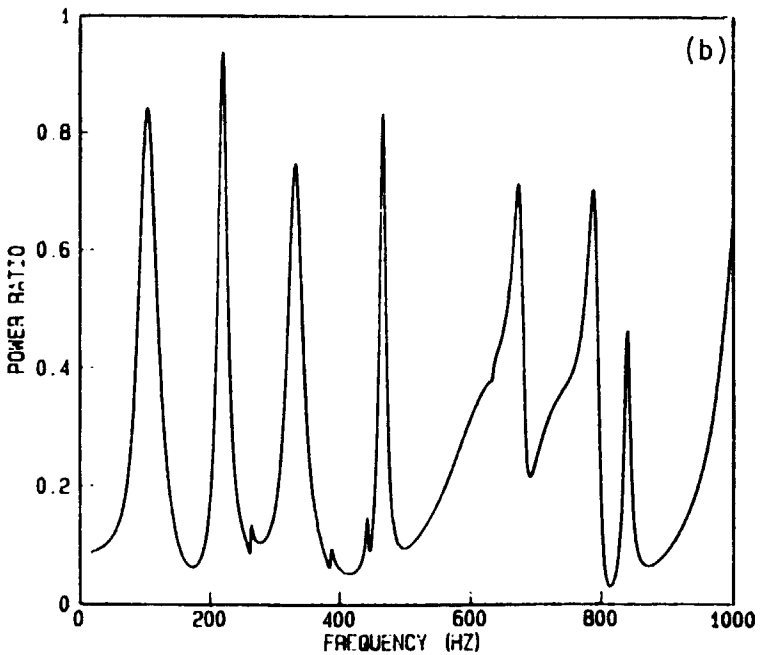

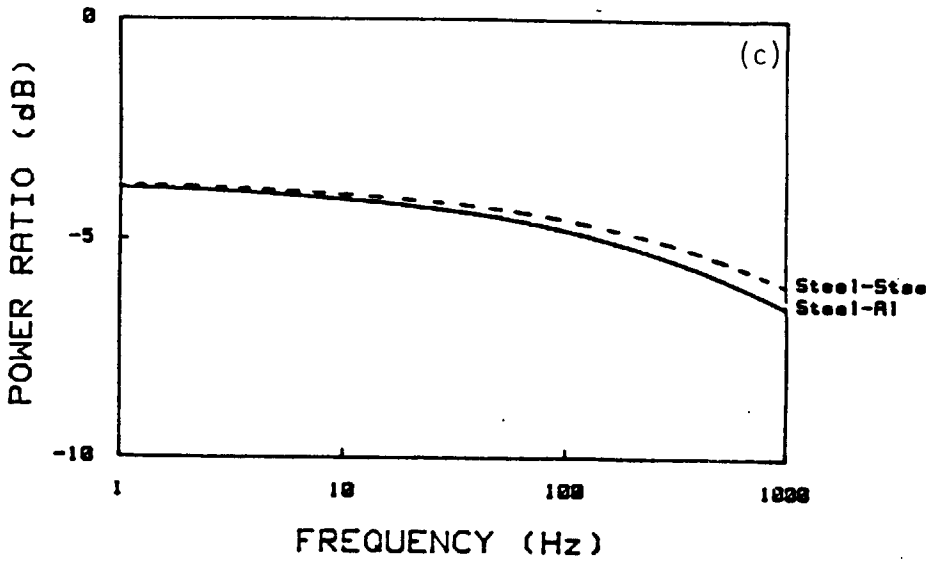

Figure 12. Power ratio for different materials, (a) Aluminium Steel: (b) steel/aluminium, both using mobility power flow approach: (c) SEA results.

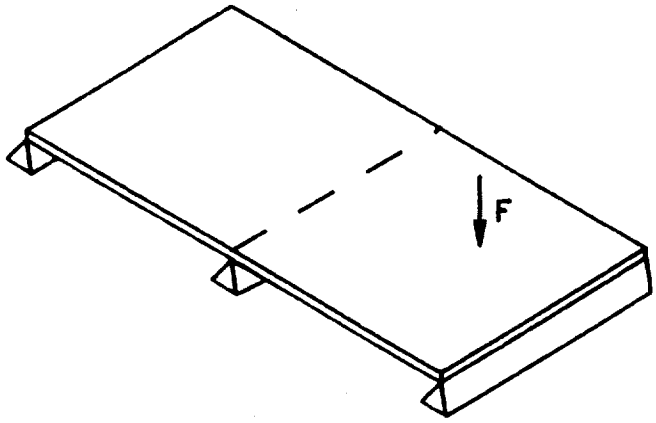

Figure 13. Alternative orientation for L-shaped plate for which the same results apply.

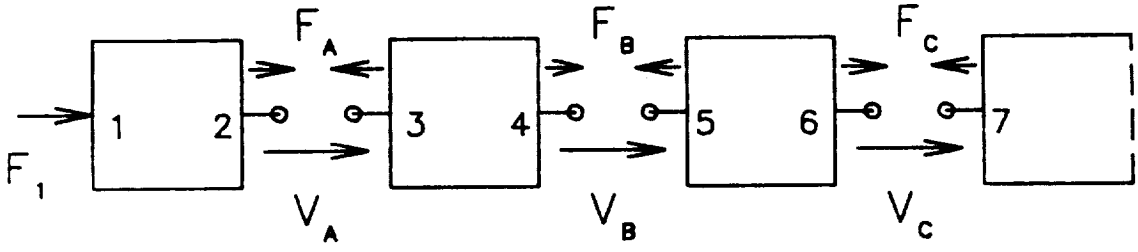

Figure 14. Model for coupled elements of a structure

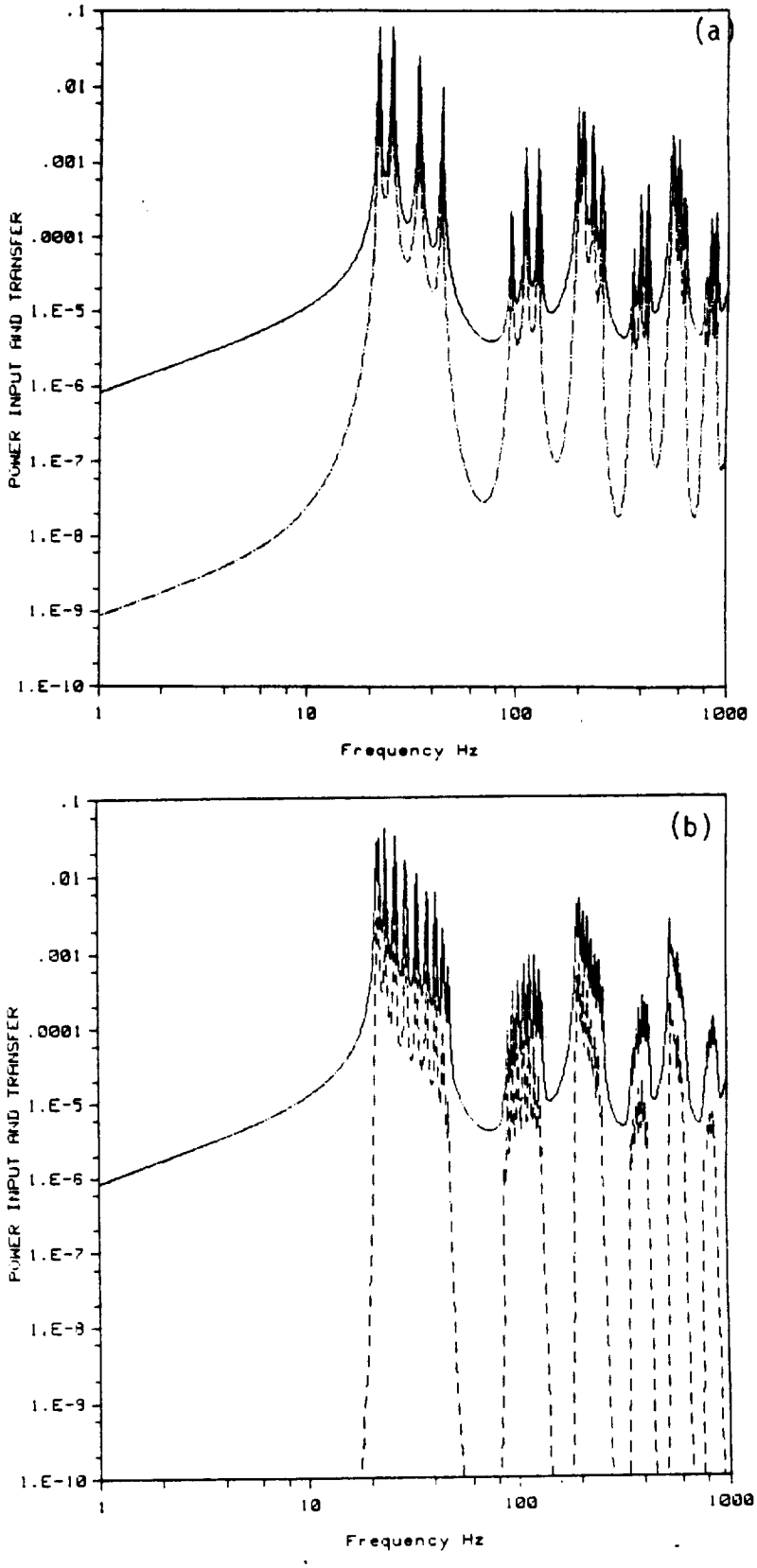

Figure 15 continues on next page.

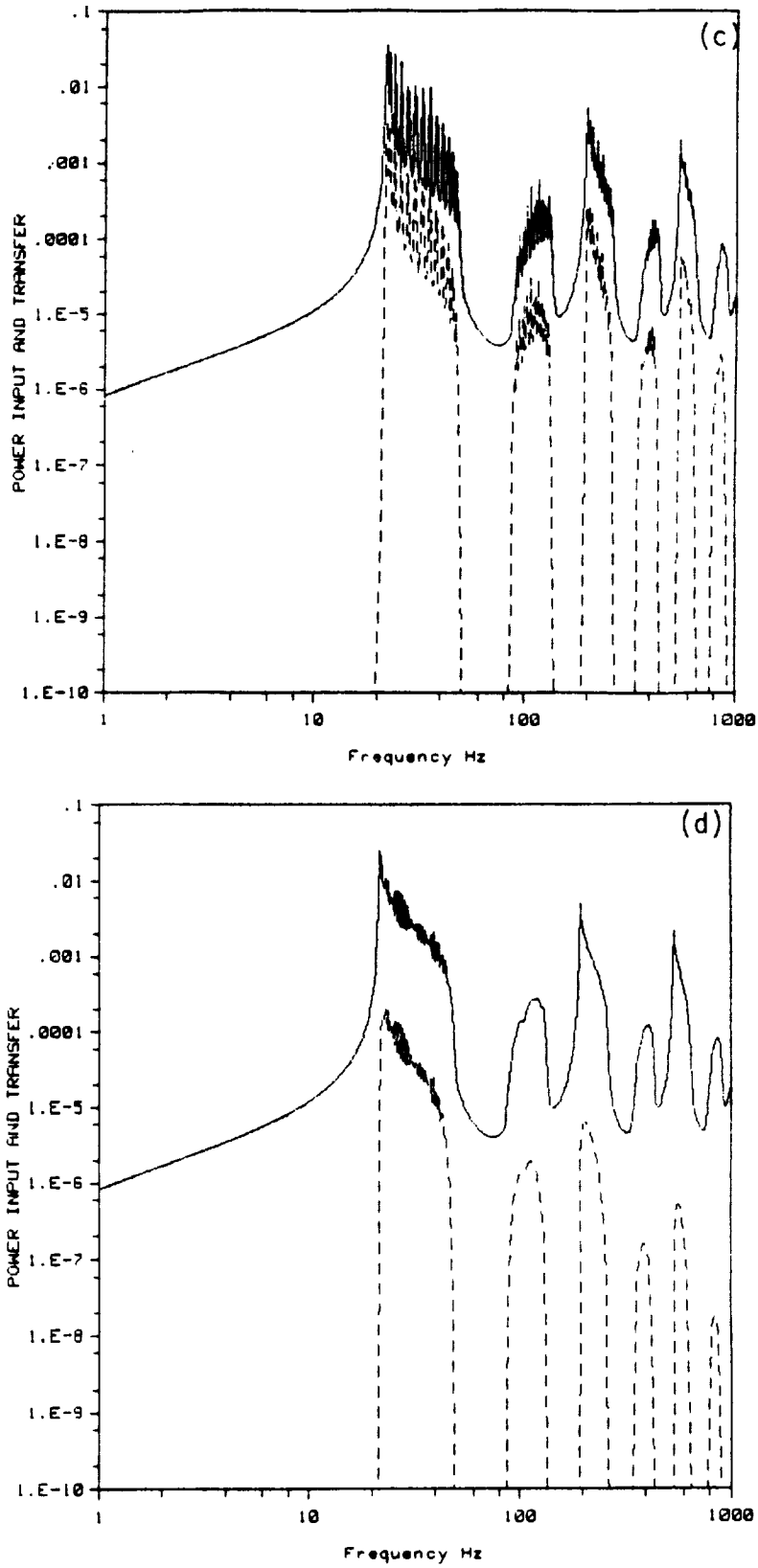

Figure 15. Power input and power transferred to last span per unit input load squared for a periodic beam on rigid supports. (a) 4 spans; (b) 10 spans; (c) 15 spans; (d) 50 spans.

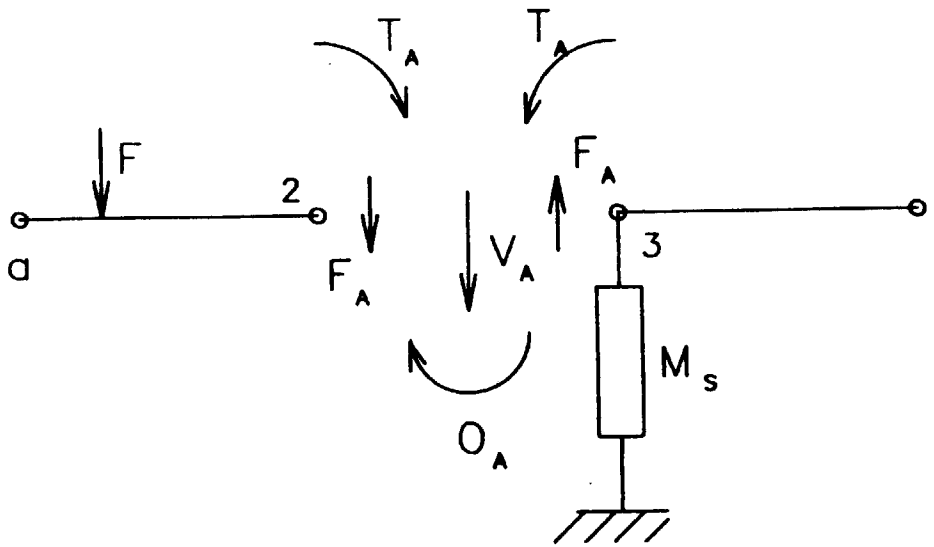

Figure 16. Model for periodic structure on flexible supports.

NASA National Aeronautics and Space Administration

Report Documentation Page

1. Report No.	2. Government Accession No.	3. Recipient's Catalog No.
NASA CR-182033		

4. Title and Subtitle
Power Flow Analysis of Two Coupled Plates with Arbitrary Characteristics

5. Report Date
June 1990

6. Performing Organization Code

7. Author(s)
J. M. Cuschieri

8. Performing Organization Report No.

10. Work Unit No.
535-03-11-03

9. Performing Organization Name and Address
Florida Atlantic University
Center for Acoustics and Vibrations
Department of Ocean Engineering
Boca Raton, FL 33431

11. Contract or Grant No.
NAG1-685

12. Sponsoring Agency Name and Address
National Aeronautics and Space Administration
Langley Research Center
Hampton, VA 23665-5225

13. Type of Report and Period Covered
Contractor Report

14. Sponsoring Agency Code

15. Supplementary Notes
Langley Technical Monitor: Vern L. Metcalf
Fourth Semi-annual Report

16. Abstract
In the last progress report (February, 88) some results were presented for a parametric analysis on the vibrational power flow between two coupled plate structures using the mobility power flow approach. The results reported then were for changes in the structural parameters of the two plates, but with the two plates identical in their structural characteristics. In this report this limitation is removed. The vibrational power input and output are evaluated for different values of the structural damping loss factor for the source and receiver plates. In performing this parametric analysis, the source plate characteristics are kept constant. The purpose of this parametric analysis is to determine the most critical parameters that influence the flow of vibrational power from the source plate to the receiver plate. In the case of the structural damping parametric analysis, the influence of changes in the source plate damping is also investigated. The results obtained from the mobility power flow approach are compared to results obtained using a Statistical Energy Analysis (SEA) approach. The significance of the power flow results are discussed together with a discussion and a comparison between the SEA results and the mobility power flow results. Furthermore, the benefits derived from using the mobility power flow approach are examined.

17. Key Words (Suggested by Author(s))	18. Distribution Statement
Aircraft noise structureborne noise acoustics vibration power flow	Unclassified - Unlimited Subject Category - 71

19. Security Classif. (of this report)	20. Security Classif. (of this page)	21. No. of pages	22. Price
Unclassified	Unclassified	46	A03

NASA FORM 1626 OCT 86